Inconsistencies in modelling interstitials in FeCr with empirical potentials

T. P. C. Klaver[1,2]*, E. del Rio[3], G. Bonny[4], S. M. Eich[5], A. Caro[6]

[1] FOM Institute DIFFER – Dutch Institute for Fundamental Energy Research, Partner in the Trilateral Euregio Cluster, Eindhoven, The Netherlands
[2] Department of Materials Science and Engineering, Delft University of Technology, Delft, The Netherlands
[3] Instituto de Fusión Nuclear, Universidad Politécnica de Madrid, Madrid, Spain
[4] SCK•CEN, Nuclear Materials Science Institute, Mol, Belgium
5 Institute of Materials Science, University of Stuttgart, Stuttgart, Germany
[6] Materials Science and Technology Division, Los Alamos National Laboratory, Los Alamos, NM 87544, USA

Abstract

We present empirical potential and Density Functional Theory results of interstitials in FeCr and pure Cr. Results show that potentials for the original and revised two-band model, a recently introduced third two-band model, and for the revised concentration-dependent model produce errors of up to multiple eV in formation and binding energies for Fe-containing interstitials in pure Cr. Fe-interstitial binding in Cr is much stronger than Cr-interstitial binding in Fe according to Density Functional Theory, but all four potentials still strongly overestimate the binding strength. At the Fe-rich end errors in empirical potentials are smaller and most of the errors are not a linear extrapolation in concentration of the larger errors in pure Cr. Interstitial formation energies in Fe-rich FeCr are underestimated by all four empirical potentials, but much less so than in pure Cr. In Fe-rich FeCr the revised concentration-dependent model produces Cr-interstitial binding energies quite similar to Density Functional Theory values, while all three two-band models show almost no binding or repulsion.

1 Introduction

FeCr is an alloy that has good properties for application as a structural material in nuclear environments. Since operating conditions like MeV neutron bombardment coming from fusion plasma can only be studied in special facilities, the alloy has been the subject of extensive atomistic modelling for over a decade. Much of the atomistic simulation work has come in the form of molecular dynamics or atomistic Monte Carlo simulations employing empirical potentials. Several FeCr potentials have been constructed explicitly in the context of radiation damage, including reproducing the change of sign in the heat of formation in Fe-rich FeCr, i.e. the original [1, 2] and revised [3] versions of the two-band model (2BM) and the revised [4] version of the concentration dependent model (CDM). These potentials represent the established state of the art for atomistic radiation damage modelling of FeCr systems too large to be handled by electronic structure methods, like Density Functional Theory (DFT).

Recently, Eich *et al* [5] published a third 2BM potential, focussing on an accurate thermodynamic description at both low and high temperature. During the construction of the original and revised 2BM and CDM, attention was focussed mostly on the Fe-rich end of the concentration range, since structural FeCr alloys consist mostly of Fe. Fitting data included Cr atoms interacting with or becoming part of self-interstitials, the archetypal point defect found in metals only after exposure to radiation. By contrast, the 3rd 2BM by Eich *et al* did not include point defect data in the fitting.

Despite the application of the original and revised 2BM potentials and the CDM potential in many studies (on topics including phase diagram prediction [e.g. 6, 7], phase separation, [e.g. 8], homogeneous [e.g. 9] and heterogeneous [e.g. 10] precipitation, short [e.g. 11, 12] and long range order [e.g. 13], impact cascades [e.g. 14-16], microstructure [e.g. 17-19], Cr-interstitial interaction [e.g. 20, 21], Cr-dislocation interaction [e.g. 22-24], dislocation-precipitate interaction [e.g. 25], grain boundary segregation [e.g. 26, 27], radiation-induced segregation [e.g. 28], point defect annealing [e.g. 29], effect of Cr concentration on vacancy stability [e.g. 4],vacancy cluster stability [e.g. 30], bubble formation [e.g. 31]) and their detailed benchmarking [32-35] to assess their strengths and weaknesses, it is still not fully known which situations they manage or fail to describe accurately. The 3rd 2BM by Eich et al has not been as extensively tested yet since its publication in 2015. Recently, we calculated interstitial formation energies with the revised CDM in FeCr alloys with 1-17 atom% Cr and found an unlikely formation energy trend that decreased with increasing Cr concentration, see below. This prompted us to investigate how accurate FeCr interstitial formation energies are reproduced at the Cr-rich end and if the energies might be 'extrapolating towards the wrong end value' in pure Cr. Having established, by comparing empirical potential and DFT results, that this is indeed the case, we determined how much of the large errors present in pure Cr are still present at concentrations in the Fe-rich end.

The build-up of this paper is as follows. In the next section a description of the computational methodology is presented. In section 3.1 CDM results are presented for interstitials in 1-17 atom% Cr, showing the aforementioned questionable formation energy trend in that concentration range. In section 3.2 we compare revised CDM and original, revised, and 3rd 2BM results for FeFe and FeCr interstitials (and Fe solutes next to vacancies) in pure Cr to DFT, showing that all four of these empirical potentials produce big errors for Fe-containing interstitials in pure Cr. Then in section 3.3 we show how much of the errors for pure Cr are still present at two Cr concentrations (8 and 16%) in the Fe-rich end. Finally, in latter part of the summary and conclusions section we briefly discuss how to improve the empirical potentials.

2 Computational details

Empirical potential calculations were performed with four different potentials obtained following two different extensions to the EAM formalism: a CDM model [36], modified to better describe the relative energy of the mixed interstitials [4]; the original [1, 2] 2BM model; the revised 2BM [3], modified to better describe

the asymmetric heat of formation of FeCr; and the 3rd 2BM, constructed to give an accurate thermodynamic description at low and high temperatures.
To relax the configurations, different MD codes were used. The CDM calculations were performed with the Large-scale Atomic/Molecular Massively Parallel Simulator (LAMMPS) classical molecular dynamics code [37]. For the original and revised 2BM calculations an in-house standard code was used. For the 3rd 2BM calculations, static energy minimization was performed using another standard MD code.
Calculations have been carried out at constant volume, relaxing the atomic positions by using the conjugate gradient algorithm [38]. Periodic boundary conditions were set for all the calculations. For the CDM, concentrations investigated are 1 to 17 atomic% Cr and pure Cr. It should be mentioned that, although the solid solution is thermodynamically unstable for concentrations above ~ 10%, these static calculations do not allow for precipitation to occur. The equilibrium lattice parameter employed in the calculations was changed as a function of Cr concentration, ranging from 2.855 Å for pure Fe to 2.878 Å for pure Cr. Different cell sizes have been used in the calculations depending on the afforded problem. Systems of 2000+1 atoms were used for the calculation of interstitial formation energies as a function of Cr concentration with the CDM. Smaller (250+1 atoms) systems were used for the interstitial formation energies at 8 and 16% Cr with empirical potentials and DFT. Systems of 250±1 atoms were used for point defects in pure Cr with empirical potentials and DFT. The point defects in pure Cr were also calculated in 2000±1 atom systems with the empirical potentials. Point defect formation energy differences between 250±1 and 2000±1 atom systems were less than 0.02 eV for vacancies and less than 0.06 eV for interstitials. In the calculation of binding energies the differences were mostly systematic and cancelled out. Therefore, system size effects can be disregarded for our purposes.
As the formation energy not only depends on the quantity of Cr atoms in the sample but also on the local position of these Cr atoms with respect to each other and to the defect, several calculations for each concentration and interstitial type were performed in the case of the study of the Cr concentration effect and also in the calculations for the 8% and 16% Cr and the mean value of the formation energy is reported.
Spin-polarised Density Functional Theory calculations were carried out using the Vienna Ab-initio Simulation Package (VASP) [39, 40]. VASP is a plane-wave DFT code that implements the Projector Augmented Wave method [41]. We used standard PAW potentials with Perdew-Wang91 parameterisation in the Generalized Gradient Approximation, that are distributed with VASP [42], with Vosko–Wilk–Nusair interpolation [43]. Fe and Cr potentials with eight and six valence electrons, respectively, were used. The plane wave energy cutoff was set to 300 eV, which is sufficient for convergence of energy differences between our systems. Brillouin zone sampling was done using 3 x 3 x 3 meshes in the Monkhorst-Pack scheme [44]. We used first order (N=1) Methfessel-Paxton smearing [45] with a smearing width of 0.3 eV.
The formation energy E_f of a system of atoms with composition Fe_nCr_m and total energy $E(Fe_nCr_m)$is calculated using

$$E_f = E(Fe_nCr_m) - nE(Fe) - mE(Cr) \quad (1)$$

where E(Fe) and E(Cr) are the energies per atom of Fe and Cr in their pure equilibrium states.
The binding energy E_b between objects (e.g., the binding energy that is released when a solute atom and a self-interstitial merge to become a mixed dumbbell) is defined as the formation energy difference between a system in which the objects are close together and a system in which the objects are far apart. Within the limited size of our systems it is not possible to separate objects over large distances. Therefore the formation energy of the situation where the objects are separated is usually calculated by calculating each object individually in a supercell. The binding energy then becomes

$$E_b = -[E_f(combined) - E_f(object1) - E_f(object2) - \ldots\ldots\ldots] \quad (2)$$

in which a positive binding energy means attraction between the objects and a negative binding energy means repulsion.

3 Results

3.1 Revised CDM interstitial formation energies in Fe-rich FeCr as a function of Cr content

Single interstitials of different types were inserted in random FeCr alloys with Cr concentrations ranging from 1-17atom% in 1% increments. Interstitials were created by deleting one by one each of the atoms in the cell and replacing them by a single interstitial (FeFe or FeCr), so that the interstitial is created in each of the possible positions in the cell. Only a given number of stable configurations are taken into account in the calculation of the medium formation energy. First, we have observed that in some cases the geometry of the final configuration does not coincide with the starting one. Second, the number of Cr atoms changes depending on the type of atom deleted (Fe or Cr) and the interstitial created (FeFe or FeCr). Only those configurations with the same initial and final geometries and a constant number of Cr atoms are used to calculate the mean formation energy for each concentration. An interstitial was deemed to have relaxed to another orientation if the angle between the original and relaxed axes of the atoms inserted as interstitials was larger than 8.1 degrees ($\cos(\alpha)<0.99$). Since we are interested in the interstitials and less in the defect-free alloy formation energy, we calculate the formation energy as 'reduced' formation energy, where the defect-free alloy formation energy has been subtracted. The result is shown in fig. 1.

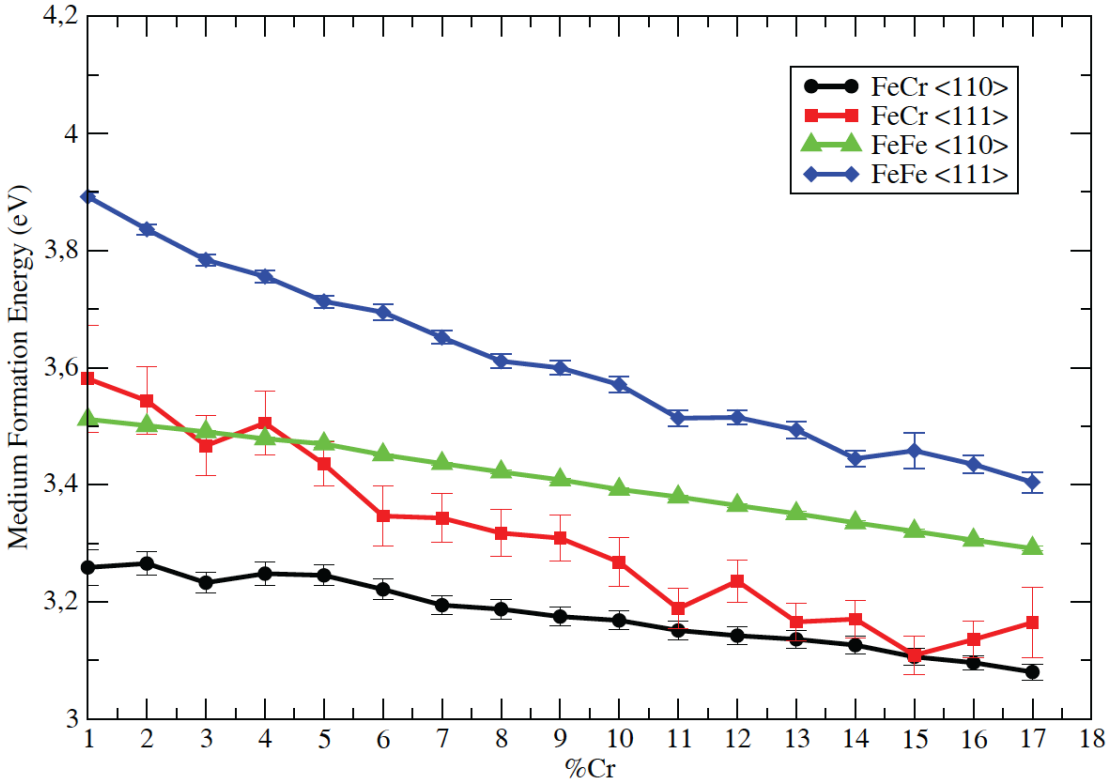

Fig. 1. Formation energies of <110> and <111> dumbbell interstitials in FeCr as a function of Cr concentration. Error bars indicate the standard error of the mean energy.

Formation energies decrease as the Cr concentration increases for all the interstitials studied. Serious fluctuations are observed for the FeCr <111> interstitial although it follows the same trend as the other interstitials. These fluctuations are likely due to the small number of configurations taken into account in calculating the mean formation energy in this case. Since only interstitials are included that do not transform during relaxation, far fewer configurations are considered for FeCr <111> interstitials than for other interstitials. This is also shown in the error bar in the figure, which is larger than for the other three interstitials studied.

The decreasing formation energy trend with increasing Cr concentration in fig. 1 seems unlikely, since interstitials in pure Cr have higher formation energies than those in pure Fe, according to DFT [46]. If the Cr concentration were further increased to the point where all atoms have become Cr, there would have to be some minimum in the formation energy at some concentration. For higher concentrations the formation energy would have to rise to the value for pure Cr. We are not aware of any phenomenon or theory that would suggest such a pattern in FeCr. Instead, the decreasing rather than increasing formation energy with increasing Cr concentration seems to indicate a problem in the revised CDM potential. This led us to the question of whether there is an error when using this potential at high Cr concentrations and if the problem also exists in other empirical potentials explicitly developed for the study of radiation damage in FeCr alloys. To investigate this, we have calculated formation and binding energies of the interstitials in pure Cr and 8% and 16%Cr with DFT and the three empirical potentials mentioned above.

3.2 Fe atoms interacting with interstitials and vacancies in pure Cr

Given that Fe-containing interstitials in pure Cr were not the focus of attention in the construction of the 2BM and CDM potentials, it is quite possible that these energies are not very well reproduced. Table I lists the formation energies of CrCr, FeFe and FeCr interstitials in pure Cr, the solution energy of a single Fe solute in pure Cr and the binding energy of one or two Fe atoms to the FeCr or FeFe dumbbell in pure Cr. Since radiation produces interstitials alongside vacancies, we also include results for Fe atoms binding to vacancies as nearest and next-nearest neighbours.

Table I. Heat of solution of an Fe solute, interstitial formation energies and Fe-to-interstitial binding energies in Cr, calculated with DFT and empirical potentials. All energies are in eV. For empirical potentials the difference to DFT energies is noted between brackets under the formation and binding energies

object	DFT		CDM		original 2BM		revised 2BM		3rd 2BM	
	E_f	E_b	E_f	E_b	E_f	E_b	E_f	E_b	E_f	E_b
Fe solute	0.44		0.45 (0.01)		-0.34 (0.78)		0.36 (0.08)		0.08 (0.36)	
CrCr <100>	6.71*		6.86 (0.15)		6.83 (0.12)		4.55 (2.16)		6.90 (0.19)	
CrCr <110>	5.66*		5.59 (0.07)		5.60 (0.06)		3.98 (1.68)		5.65 (0.01)	
CrCr <111>	5.70*		5.60 (0.10)		5.62 (0.08)		4.05 (1.65)		5.67 (0.03)	
FeCr <100>	6.27	0.88	un-stable		3.49 (2.78)	3.00 (2.12)	3.84 (2.43)	1.07 (0.19)	un-stable	
FeCr <110>	5.00	1.10	3.72 (1.28)	2.33 (1.23)	3.52 (1.48)	1.74 (0.64)	3.72 (1.28)	0.62 (0.48)	un-stable	
FeCr <111>	5.37	0.77	4.12 (1.25)	1.92 (1.15)	3.50 (1.87)	1.78 (1.01)	3.85 (1.52)	0.56 (0.21)	3.74 (1.63)	2.01 (1.24)
FeFe <100>	5.98	1.61	3.83 (2.15)	3.93 (2.32)	2.94 (3.04)	3.21 (1.60)	3.98 (2.00)	1.29 (0.32)	3.74 (2.24)	3.32 (1.71)
FeFe <110>	4.45	2.09	3.58 (0.87)	2.92 (0.83)	2.65 (1.80)	2.27 (0.18)	3.41 (1.04)	1.29 (0.80)	3.34 (1.11)	2.47 (0.38)
FeFe <111>	5.07	1.51	4.09 (0.98)	2.41 (0.90)	2.78 (2.29)	2.16 (0.65)	3.64 (1.43)	1.13 (0.38)	3.39 (1.68)	2.44 (0.93)
pure Cr vacancy	2.74		2.56 (0.18)		2.56 (0.18)		2.52 (0.22)		2.56 (0.18)	
Fe nearest neighb. to vacancy	2.82	0.36	2.50 (0.32)	0.51 (0.15)	2.18 (0.64)	0.04 (0.32)	2.76 (0.06)	0.12 (0.24)	2.55 (0.27)	0.09 (0.27)
Fe next nearest neighb. to vacancy	2.98	0.20	2.47 (0.51)	0.54 (0.34)	2.18 (0.80)	0.04 (0.16)	2.78 (0.20)	0.10 (0.10)	2.60 0.38)	0.04 (0.16)

* data taken from [47]

It is immediately obvious from Table I that all four empirical potentials produce large errors for Fe-containing interstitials. All formation energies are underestimated by one or several eV, while binding energies for the CDM and

original and 3rd 2BM are systematically overestimated (if even stable, for the 3rd 2BM) by tenths of eV or full eVs. For the revised 2BM the errors in the binding of Fe atoms to interstitials are smaller in absolute value, but formation energies of CrCr interstitials are too low. For the CDM, the formation energy is underestimated by almost the same energy that the binding energy is overestimated, in contrast to the 2BMs. This means that fixing the errors in the CDM might be easier than for the 2BMs, as for the CDM correcting the binding energy might be enough to correct the formation energy too. While the largest errors occur for the mostly theoretical <100> dumbbells, many of the more relevant <110> and <111> interstitial energies also have large errors.
Results for Fe atoms binding to vacancies as nearest and next –nearest neighbours also show errors although smaller than in the case of interstitials. Again, all the formation energies are underestimated with the revised 2BM providing quite good values. In contrast, binding energies are overestimated for the CDM and underestimated for the 2BMs by tenths of eV.
We have checked if magnetic moments on the atoms inside and next to the interstitials can help explain the DFT results in Table I, in a similar way that they can help explain energies of some interstitial and defect-free configurations in Fe-rich FeCr [47, 48]. However, this analysis proved inconclusive.

3.3 Cr-interstitial binding energies at 8 and 16 atom% Cr

If an error of multiple eV in pure Cr is interpolated to ~10% Cr, the error would still be tenths of eV. The binding between Cr atoms and interstitials in Fe-rich FeCr is hundredths or a few tenth of an eV [46], so the error could outweigh legitimate Cr-interstitial interactions. In order to test if this is indeed the case, two sets of 20 different configurations of 5x5x5 bcc cells systems with both 8 and 16% Cr were calculated. The first set at each concentration consisted of supercells with an FeFe <110> dumbbell interstitial and randomly distributed Cr solutes. In the second set, one Cr solute some distance away from the interstitial was exchanged with an Fe atom inside the interstitial, creating a mixed dumbbell. This allows us to have a constant number of Cr atoms in the sample and therefore the Cr concentration is the same for both interstitials, FeFe and FeCr. In both sets the ionic positions were relaxed. The energy difference between two such relaxed configurations is taken as the binding energy of the Cr atom to the interstitial. Results averaged over the 20 configurations are shown in table II.

Table II. Formation energies, formation energy differences and binding energies, averaged over 20 configurations, for defect-free systems and systems with FeFe and FeCr <110> interstitials, inside 8 and 16% Cr FeCr random alloys. Below the interstitial formation and binding energies, the standard errors are noted between brackets. All energies are in eV.

8% Cr	E_f, defect-free	E_f, FeFe interst.	E_f, FeFe interst. – E_f, defect-free	E_f, FeCr interst.	E_f, FeCr interst. – E_f, defect-free	E_b Cr-to-interst.
DFT	0.73	4.77 (0.03)	4.04	4.45 (0.03)	3.72	0.32 (0.03)
revised CDM	0.73	4.13	3.40	3.75	3.02	0.38

		(0.02)		(0.06)		(0.06)
original 2BM	0.41	3.86 (0.02)	3.45	3.83 (0.03)	3.42	0.03 (0.03)
revised 2BM	0.56	4.12 (0.02)	3.56	4.10 (0.02)	3.54	0.02 (0.02)
3rd 2BM	0.24	3.63 (0.08)	3.39	3.58 (0.08)	3.34	0.05 (0.03)
16% Cr	E_f, defect-free	Ef, FeFe interst.	E_f, FeFe interst. – E_f, defect-free	E_f, FeCr interst.	E_f, FeCr interst. – E_f, defect-free	E_b Cr-to-interst.
DFT	5.27	9.10 (0.04)	3.83	8.89 (0.03)	3.62	0.21 (0.04)
revised CDM	5.80	9.34 (0.04)	3.54	9.08 (0.05)	3.28	0.26 (0.05)
original 2BM	4.31	7.70 (0.02)	3.39	7.81 (0.05)	3.50	-0.11 (0.03)
revised 2BM	4.64	8.17 (0.02)	3.53	8.29 (0.05)	3.65	-0.12 (0.03)
3rd 2BM	4.41	7.64 (0.09)	3.23	7.76 (0.10)	3.35	-0.12 (0.03)

Interpreting the formation energies in table II is slightly less straightforward than interpreting those for pure Cr, as in 8 and 16% Cr alloys, the formation energy of the alloy without any interstitial contributes part of the formation energy. Again, as we are interested in the interstitials and less in the defect-free alloy formation energy, we focus our attention on 'reduced' formation energies (see section 3.1).

With the exception of the revised 2BM FeCr dumbbell energy in the 16% Cr alloy, the reduced formation energies are systematically underestimated by tenths of eV. The revised 2BM has the smallest differences to DFT results. The systematic underestimation of the formation energies is consistent with results obtained for pure Cr. However, the binding energies are very different from the results for pure Cr. None of the three potentials give a strong overestimation of the binding energy, as was found in pure Cr. The CDM gives surprisingly good results at both concentrations, correctly reproducing the non-linear pattern of the binding energy as a function of Cr concentration as well as being close in absolute value for both concentrations. By contrast, the 2BMs give almost no binding at 8% Cr and repulsion at 16% Cr.

Curiously, when going from 8 to 16% Cr, the reduced DFT formation energy slightly decreases. This is in line with revised CDM results in section 3.1 and therefore much against expectations and against the considerations that originally lead us to look at Fe-containing interstitials in pure Cr. It suggests there is a minimum in the interstitial formation energy, as predicted by the CDM. At present we have no good explanation as to why that would be.

4 Summary and conclusions

We have calculated formation and binding energies of interstitials in pure Cr and $Fe_{230}Cr_{21}$ and $Fe_{210}Cr_{41}$ alloys with DFT and four empirical potentials. Results show large errors up to multiple eV for interstitial energies in pure Cr for all four potentials. The largest of these errors are due to overly strong binding of Fe to interstitials for the original 2BM and revised CDM and due to too low formation energies of CrCr interstitials for the revised 2BM. For the 3rd 2BM, errors are largely due to overbinding of Fe to the interstitial as for the original 2BM and revised CDM, but for the 3rd 2BM some mixed interstitials in Cr are also unstable. Interestingly, the 3rd 2BM potential often predicts energies close to the other two 2BMs, following the trend of the original 2BM potential, although no point defects were directly included in the construction. This could be explained by the fact that the optimization for the 3rd 2BM was initialized using the parameter values of the original 2BM potential, possibly keeping some of its properties. DFT shows that one Fe atom binds to interstitials in Cr by ~1 eV and two Fe atoms bind by up to 2 eV, much stronger than Cr atoms bind to interstitials in Fe [46]. However, the original and 3rd 2BM and revised CDM empirical potentials still overestimate the Fe-interstitial binding in Cr, sometimes by several eV, while the revised 2BM potential underestimates it by tenths of eV.
In order to assess whether the large errors in pure Cr extrapolate to Fe-rich FeCr, we have performed calculations on several FeCr configurations for the FeFe and FeCr <110> interstitial for 8% and 16%Cr concentrations. We found that some of the DFT results and empirical potential errors in pure Cr extrapolate down in concentration to the Fe-rich end while others do not. The underestimation of the formation energy by empirical potentials is also present in most cases at 8 and 16% Cr. For most cases the 'reduced' interstitial formation energy is also underestimated. On the other hand, the overly strong solute-interstitial binding is not present at 8 and 16 % Cr. The revised CDM reproduces the DFT binding energy surprisingly well at both concentrations, while the 2BMs show hardly any binding at 8% and repulsion at 16%. The average binding is also not linear in Cr concentration, being 0.32 eV at 8% Cr and 0.21 eV at 16% Cr (and 1.10 eV in pure Cr), according to DFT.
From the point of view of using empirical potentials to accurately model radiation damage in FeCr, results presented in this work, especially those for pure Cr, have to be regarded as unwelcome news. Due to the lack of attention to interstitials in pure Cr during construction of the potentials, large errors are present at the Cr-rich end. A first attempt to remedy this situation might be to refit the potentials with some of the DFT data for pure, 8 and 16% Cr included in the fitting procedure. However, the 'manouvering room' available from the fit parameters within the empirical potential models is limited and for the revised 2BM it was already almost fully used. Improving the situation in pure Cr and at 8 and 16% would likely come at the expense of reproducing other properties less accurately. Solving the known errors without making other results worse is likely to require the more rigorous step of changing the model.

Acknowledgements

This work was carried out with financial support from NWO. AC gratefully acknowledges the support of the US Department of Energy (DOE) through the

LANL/LDRD Program. The research leading to these results is partly funded by the European Atomic Energy Community's (Euratom) Seventh Framework Programme FP7/2007-2013 under grant agreement No. 604862 (MatISSE project) and contributes to the Joint Programme on Nuclear Materials (JPNM) of the European Energy Research Alliance (EERA). This work has partially been founded by the Deutsche Forschungsgemeinschaft (grant no. SCHM 1182/13). Research by EdR has been carried out within the framework of the EUROfusion Consortium and has received funding from the Euratom research and training programme 2014-2018 under grant agreement Nº 633053 and WPENR: Enabling Research, IFE, Project: AWP15-ENR-01/CEA-02. The views and opinions expressed herein do not necessarily reflect those of the European Commission. EdR was also supported by the Spanish Ministry of Economy and Competitiveness project RADIAFUS ENE2012-39787-C06-03, Comunidad de Madrid (S2013/MAE-2745 "TECHNOFUSION(II)-CM"). EdR acknowledges the computer resources and technical assistance provided by the Centro de Supercomputación y Visualización de Madrid (CeSViMa).

References

*klaver2@gmail.com

1 P. Olsson, J. Wallenius, C. Domain, K. Nordlund, L. Malerba, Phys. Rev. B 72 (2005) 214119
2 P. Olsson, J. Wallenius, C. Domain, K. Nordlund, L. Malerba, Phys. Rev. B 74 (2006) 229906(E)
3 G. Bonny, R. C. Pasianot, D. Terentyev, L. Malerba, Philos. Mag. 91 (2011) 1724
4 E. del Rio, J. M. Sampedro, H. Dogo, M. J. Caturla, M. Caro, A. Caro, J. M Perlado, J. Nucl. Mater. 408 (2011) 18
5 S. M. Eich, D. Beinke, G. Schmitz, Comp. Mater. Sci. 104 (2015) 185
6 G. Bonny, R. C. Pasianot, E. E. Zhurkin, M. Hou, Comp. Mater. Sci. 50 (2011) 2216
7 G. Bonny, R. C. Pasianot, L. Malerba, A. Caro, P. Olsson, M.Yu. Lavrentiev, J. Nucl. Mater. 385 (2009) 268
8 C. Pareige, M. Roussel, S. Novy, V. Kuksenko, P. Olsson, C. Domain, P. Pareige, Acta Mater. 59 (2011) 2404
9 G. Bonny, D. Terentyev, L. Malerba, D. Van Neck, Phys. Rev. B. 79 (2009) 104207
10 A. Caro, M. Caro, P. Klaver, B. Sadigh, E. M. Lopasso, S. G. Srinivasan, JOM 59 (2007) 52
11 G. Bonny, P. Erhart, A. Caro, R. C. Pasianot, L. Malerba, M. Caro, Modelling Simul. Mater. Sci. Eng. 17 (2009) 025006
12 P. Erhart, A. Caro, M. Serrano de Caro, B. Sadigh, Phys. Rev. B 77 (2008) 134206
13 C. Pareige, C. Domain, P. Olsson, J. Appl. Phys. 106 (2009) 104906
14 D. Terentyev, K. Vörtler, C. Björkas, K. Nordlund, L. Malerba, J. Nucl. Mater. 417 (2011) 1063
15 D. A. Terentyev, L. Malerba, R. Chakarova, K. Nordlund, P. Olsson, M. Rieth, J. wallenius, J. Nucl. Mater. 349 (2006) 119

16 C. Björkas, K. Nordlund, L. Malerba, D. Terentyev, P. Olsson, J. Nucl. Mater. 372 (2008) 312
17 D. Terentyev, P. Olsson, L. Malerba, J. Nucl. Mater. 386-388 (2009) 140
18 D. Terentyev, P. Olsson, L. Malerba, A.V. Barashev, J. Nucl. Mater. 362 (2007) 167
19 D. Terentyev, L. Malerba, A. V. Barashev, Phil. Mag. 88 (2008) 21
20 D. Terentyev, P. Olsson, T. P. C. Klaver, L. Malerba, Comp. Mater. Sci. 43 (2008) 1183
21 L. Gamez, B. Gamez, M. J. Caturla, D. Terentyev, J. M. Perlado, Nucl. Instrum. Meth. B 269 (2011) 1684
22 D. Terentyev, A. Bakaev, J. Phys.: Condens. Matter 25 (2013) 265702
23 D. A. Terentyev, G. Bonny, L. Malerba, Acta Mater. 56 (2008) 3229
24 D.A. Terentyev, L. Malerba, Comp. Mat. Sci. 43 (2008) 855
25 D. Terentyev, G. Bonny, C. Domain, R. C. Pasianot, Phys. Rev. B 81 (2010) 214106
26 D. Terentyev, X. He, E. Zhurkin, A. Bakaev, J. Nucl. Mater. 408 (2011) 161
27 G. Bonny, D. Terentyev, L. Malerba, J. Nucl. Mater. 385 (2009) 278
28 J. P. Wharry, G. S. Was, Acta Mater. 65 (2014) 42
29 D. Terentyev, N. Castin, C. J. Ortiz, J. Phys.: Condens. Matter 24 (2012) 475404
30 J. M. Sampedro, E. del Rio, M. J. Caturla, A. Caro, M. Caro, J. M. Perlado, Nucl. Instrum. Meth. B 303 (2013) 46
31 A. Caro, J. Hetherly, A. Stukowski, M. Caro, E. Martinez, S. Srivilliputhur, L. Zepeda-Ruiz, M. Nastasi, J. Nucl. Mater. 418 (2011) 261
32 L. Malerba, A. Caro, J. Wallenius, J. Nucl. Mater. 382 (2008) 112
33 G. Bonny, R. C. Pasianot, L. Malerba, A. Caro, P. Olsson, M. Yu. Lavrentiev, J. Nucl. Mater. 385 (2009) 268
34 T. P. C. Klaver, G. Bonny, P. Olsson, D. Terentyev, Modelling Simul. Mater. Sci. Eng. 18 (2010) 075004
35 J. M. Sampedro, E. del Rio, M. J. Caturla, M. Victoria, J. M. Perlado, J. Nucl. Mater. 417 (2011) 1050
36 A. Caro, D. A. Crowson, M. Caro, Phys. Rev. Lett. 95 (2005) 075702
37 S. Plimpton, J. Comp. Phys., 117 (1995) 1 http://lammps.sandia.gov
38 W.H. Press, S.A. Teukolsky, W.T. Vetterling, B.P. Flannery, Numerical Recipes in Fortran 77: the Art of Scientific Computing, 2nd ed., Cambridge University Press, 1992.
39 G. Kresse, J. Hafner, Phys. Rev. B 47 (1993) RC558
40 G. Kresse, J. Furthmuller, Phys. Rev. B 54 (1996) 11169
41 P. E. Blöchl, Phys. Rev. B 50 (1994) 17953
42 G. Kresse, D. Joubert, Phys. Rev. B 59 (1999) 1758
43 S. H. Vosko, L. Wilk, M. Nusair, Can. J. Phys. 58 (1980) 1200
44 H. J. Monkhorst, J. D. Pack, Phys. Rev. B 13 (1976) 5188
45 M. Methfessel, A. T. Paxton, Phys. Rev. B 40 (1989) 3616
46 P. Olsson, C. Domain, J. Wallenius, Phys. Rev. B 75 (2007) 014110
47 P. Olsson, C. Domain, J. Wallenius, Phys. Rev. B 75 (2007) 014110
48 T. P. C. Klaver, R. Drautz, M. W. Finnis, Phys. Rev. B 74 (2006) 094435